

Orientational order and solid-liquid coexistence in the two-dimensional Lennard-Jones system

C. Udink

Laboratory for Physical Chemistry, University of Amsterdam, Nieuwe Achtergracht 127, 1018 WS Amsterdam, The Netherlands

D. Frenkel

FOM-Institute for Atomic and Molecular Physics, P.O. Box 41883, 1009 DB Amsterdam, The Netherlands

(Received 22 December 1986)

There exist large discrepancies between the results of different techniques used to locate the melting point of a two-dimensional Lennard-Jones system. In particular, the melting line determined by Barker *et al.* [Physica **106A**, 226 (1981)] through thermodynamic integration differs from the limit of mechanical stability of the two-dimensional (2D) solid which follows from recent simulations on very large systems. This discrepancy is puzzling because in the latter simulations no hysteresis was observed. We report a new calculation of the relevant part of the melting line of a 2D Lennard-Jones system by thermodynamic integration. Our results differ significantly from the results reported by Barker *et al.* and agree well with the simulations on large systems. We note that the structural properties of the two-phase region for a large system [$O(10^4)$ particles] exhibit all the characteristics of a bond-orientational order-disorder transition. This suggests that solid-liquid coexistence in 2D may differ qualitatively from its three-dimensional counterpart.

I. INTRODUCTION

Over the last few years, there has been considerable interest in computer simulations of the two-dimensional melting transition. The renewed interest in this subject was inspired by the theoretical predictions of Kosterlitz and Thouless¹ and the remarkable extension of the Kosterlitz and Thouless theory formulated by Nelson and Halperin² and Young.³ The latter authors proposed that the melting transition in two dimensions might follow a scenario that differs qualitatively from its three-dimensional counterpart. In particular, Halperin, Nelson, and Young argued that two-dimensional melting might proceed through two continuous transitions, rather than a single first-order phase transformation. In the Kosterlitz-Thouless, Halperin, Nelson-Young (KTHNY) theory, the two-dimensional (2D) solid, which has quasi-long-range translational order and true long-range bond-orientation order, first melts to a fluid phase, which has short-range translational order and quasi-long-range bond-orientational order. The nature of the bond order depends on the symmetry of the solid phase. For 2D solids with a sixfold symmetry, the intermediate fluid phase has sixfold quasi-long-range bond order. Such a phase is referred to as a "hexatic" phase. A second phase transition is needed to transform the hexatic fluid into a normal isotropic fluid with short-range translational and orientational order. The KTHNY theory makes a number of very specific, and partly universal, predictions about the critical behavior of the correlation functions of the translational and orientational order parameters in the vicinity of these two phase transitions. Much of the subsequent computational effort⁵ was aimed at verifying the KTHNY predictions for specific model systems. The first model system to be investigated was the two-dimensional Lennard-Jones system. The initial simulations of Frenkel and McTague⁵ seemed to support the KTHNY predictions, although a

single first-order phase transition could not be ruled out. Subsequently, some authors reported simulations that provided evidence in line with the KTHNY picture,⁶ while (most) others⁷⁻⁹ concluded that the melting transition in the 2D Lennard-Jones (LJ) system was a normal first-order phase transformation.

If at present the second point of view prevails, this is mainly due to two rather different sets of simulations, which both supported the first-order scenario. Part of the evidence comes from simulations of Abraham,⁷ who studied the 2D LJ system along an isobar, and found evidence for discontinuous jumps in the density and hysteresis typical for a first-order phase transition. The complete melting line of the 2D LJ system was thereupon calculated by Barker, Henderson, and Abraham.¹⁰ Barker *et al.* computed the absolute free energy of the solid and fluid phases and used this information to locate the coexistence points. The resulting phase diagram is qualitatively similar to the phase diagram of the 3D Lennard-Jones system.¹¹

Complementary evidence for first-order melting in the 2D LJ system comes from the simulations of Bakker *et al.*¹² These authors carried out extensive simulations of large (up to 16 000 particles) two-dimensional Lennard-Jones systems, along an isochore. Bakker *et al.* did not compute the thermodynamic melting point, but focused on the behavior of the bond-order correlation function. Their simulations suggest that the bond-order correlation length in the isotropic fluid phase does not diverge as predicted by the KTHNY theory (it is supposed to grow as $\exp[b/(T - T^*)^{1/2}]$, as the transition to the hexatic phase at temperature T^* is approached), but saturates at a large but finite value.

Surprisingly, although the simulations of Refs. 10 and 12 agree about the first-order nature of the 2D melting transition, they appear to yield different values for the melting point of the solid. In particular, Barker *et al.*

predicted that the solid will melt at a temperature that is some 25% lower than observed by Bakker *et al.* (see Fig. 1). It should be noted that this discrepancy is too large to be accounted for by finite-size effects or hysteresis (which, incidentally, was not observed in Ref. 12). Moreover, this discrepancy may have implications for the stability of the solid at melting. One of the results of the KTHNY theory is that melting through dislocation unbinding must take place if the 'stiffness' constant K , defined as

$$K = (4a^2/kT)[\mu(\mu + \lambda)/(2\mu + \lambda)]$$

(where μ and λ are the elastic Lamé coefficients of the 2D solid and a is the lattice spacing), becomes less than 16π . According to Abraham,⁷ $K/16\pi$ is appreciably larger than 1 at the thermodynamic melting point. The implication is that before the transition from the solid to hexatic phase can occur, a normal first-order melting transition must intervene. In contrast, Tobochnik and Chester⁶ found, in constant density simulations on the same model system, that the criterion $K = 16\pi$ is well satisfied at the temperature where the solid phase is observed to melt. However, the latter simulations did not determine the thermodynamic melting line, and it might be argued that the simulations in Ref. 6 locate the limit of mechanical rather than thermodynamical stability of the solid. What is worrisome, however, is that the subsequent simulations by Bakker *et al.*¹² and Udink *et al.*¹³ on systems of more than 10 000 particles, both find a melting temperature that

is in better agreement with the data of Tobochnik and Chester than those of Barker *et al.* (see Fig. 1).

In 1981, Toxvaerd⁸ recomputed the melting transition of the 2D LJ system for one reduced temperature ($T^* = 1$). This author concluded that the two-phase region was narrower than estimated in Ref. 1. In addition, he found evidence for a noticeable system size dependence of the width of the two-phase region. However, the melting density found by Toxvaerd differed even more from the results on the large systems^{12,13} than the one found by Barker *et al.*

In order to gain a better understanding of the melting behavior in large 2D LJ systems, as reported in Ref. 13, we have carried out a new calculation of part of the melting line, using a different method to compute the free energy of the solid. As we shall show below, this method leads to an estimate of the thermodynamic melting line that is in better agreement with the results for large system sizes.^{12,13} In addition, the present results lead to a better understanding of the implications of the simulations reported in Ref. 13.

II. CALCULATIONS

We performed constant-density Monte Carlo simulations of a system with 240 particles, along the two isotherms $T^* = 0.83$ and $T^* = 1.00$. The results are given in the following reduced units: $p^* = p\sigma^2/\epsilon$, $T^* = k_B T/\epsilon$, and $\rho^* = \rho\sigma^2$. In these units the cutoff radius is $r_c^* = r_c/\sigma = 3.367$. In the calculations, a tail correction in the pressure and in the potential energy was included. However we checked that our final result was not sensitive to the presence or absence of this correction as long as it was treated consistently in both phases. The equation of state for the fluid branch was obtained by compressing from low densities ($\rho^* = 0.09$). The data for the solid were obtained by expansion from a high density ($\rho^* = 0.9165$). The data for both isotherms have been collected in Table I. The present data can be compared with those of Ref. 10. The agreement is excellent; the differences are less than the indicated errors. This is also the case for the potential energies (not listed in Table I).

The free-energy calculation is performed in the following way. First of all, we need to know the free energy of the solid reference states: $(\rho^*, T^*) = (0.9165, 0.83)$ and $(\rho^*, T^*) = (0.9165, 1.00)$. The determination of these free energies is described in Appendix A. Using this procedure, we obtain the following estimates for the excess free energy per particle of a 240-particle LJ crystal at a density $\rho^* = 0.9165$ and temperatures $T^* = 1.0$ and $T^* = 0.83$: $\beta F_{ex}(T^* = 1.0) = 0.914(1)$ and $\beta F_{ex}(T^* = 0.83) = 0.375(3)$, where the number between brackets indicates the estimated error in the last digit. Comparing these values to the corresponding ones in Ref. 10, namely $\beta F_{ex}(T^* = 1.0) = 0.951$ and $\beta F_{ex}(T^* = 0.83) = 0.419$, we note that the latter are systematically higher. The same holds for the value $\beta F_{ex}(T^* = 1.0) = 0.947(3)$ computed by Toxvaerd.⁸ In addition, as we shall show below, the data of Refs. 9 and 10 are also significantly higher than those obtained from a direct thermodynamic integration through the "van der Waals loop" in the solid-fluid coex-

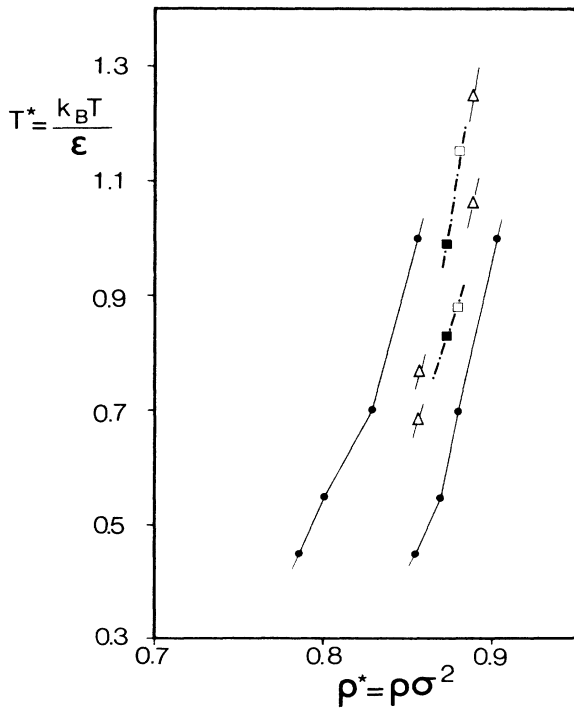


FIG. 1. Compilation of computer simulation results for the melting line of the two-dimensional Lennard-Jones system plotted in the (ρ^*, T^*) plane. The dots connected by the solid line: Barker *et al.*, open triangles (two densities): Tobochnik *et al.*; open squares: Bakker *et al.*; solid squares: Udink *et al.*

TABLE I. Results of the Monte Carlo simulation ($N=240$).

$T^*=0.83$			$T^*=1.00$		
ρ^*	p^*		ρ^*	p^*	
0.948	0.06946 ± 0.00017	liquid	0.0978	0.08951 ± 0.0003	
0.0959	0.06817 ± 0.00013		0.2223	0.19506 ± 0.0007	
0.2156	0.13521 ± 0.00081		0.3427	0.3146 ± 0.002	
0.2182	0.1389 ± 0.00069		0.4556	0.4749 ± 0.005	
0.3323	0.2005 ± 0.0023		0.5584	0.7436 ± 0.008	
0.3363	0.2029 ± 0.0025		0.6488	1.2152 ± 0.0135	
0.4418	0.291 ± 0.004		0.7247	2.027 ± 0.011	
0.4471	0.290 ± 0.007		0.7844	3.119 ± 0.032	
0.5415	0.437 ± 0.008		0.8266	4.247 ± 0.01	
0.5480	0.446 ± 0.013		0.8504	5.131 ± 0.029	
0.6291	0.702 ± 0.013		0.856	5.27 ± 0.1	
0.6366	0.745 ± 0.013		0.86	5.13 ± 0.11	
0.7027	1.190 ± 0.013		0.87	5.06 ± 0.13	
0.7111	1.272 ± 0.016		0.88	5.14 ± 0.10	
0.7606	1.906 ± 0.016				
0.7697	2.033 ± 0.019				
0.8015	2.740 ± 0.02				
0.8111	2.908 ± 0.036				
0.8246	3.198 ± 0.021				
0.8345	3.477 ± 0.048				
0.85	3.629 ± 0.061				
0.86	3.694 ± 0.058				
0.87	3.965 ± 0.022				
0.88	4.1 ± 0.1				
		Solid			
0.9165	5.338 ± 0.016		0.9165	6.43 ± 0.023	
0.9	4.521 ± 0.02		0.91	6.15 ± 0.039	
0.89	4.095 ± 0.023		0.903	5.76 ± 0.042	
0.88	3.751 ± 0.03		0.89	5.16 ± 0.046	
0.87	3.389 ± 0.028		0.88	4.81 ± 0.025	
0.86	3.205 ± 0.051				

istence region.

A possible explanation for the small but significant difference between the present results for the free energy and those obtained in Refs. 9 and 10 is the following. When evaluating the excess free energy of a finite ($N=240$) Lennard-Jones crystal with fixed center of mass, we are careful to use an ideal-gas reference system of the same number of particles and fixed center of mass. It is likely that this procedure leads to results that are less dependent on system size than the data presented in Refs. 9 and 10.

The next step is to locate the solid-liquid coexistence point using the computed free energies and equation of state data of Table I. The technical details are discussed in Appendix B. Here we just note that the procedure, which we (and Refs. 9 and 10) followed is biased in one respect: we assume that the solid and fluid equations of states can be fitted to smooth monotonic functions of the density in the vicinity of the phase transition. Such an approach is only permissible if one expects a first-order phase transition. The equation-of-state data for the 240-particle system given in Table I appear compatible with this assumption. The resulting solid-liquid coexistence points are shown in Figs. 2 and 3. The solid-liquid coex-

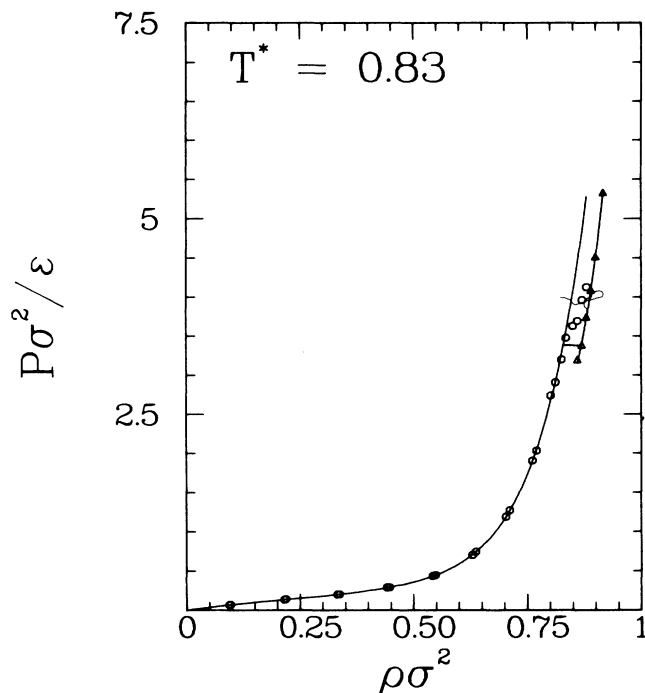


FIG. 2. Monte Carlo results for the isotherm of a 240-particle 2D LJ system at $T^*=0.83$. The dots are calculations of the fluid branch; the triangles of the solid branch. The lines are polynomial fits discussed in Appendix B. The resulting tieline of the coexistence region is given by the horizontal line (see Table II).

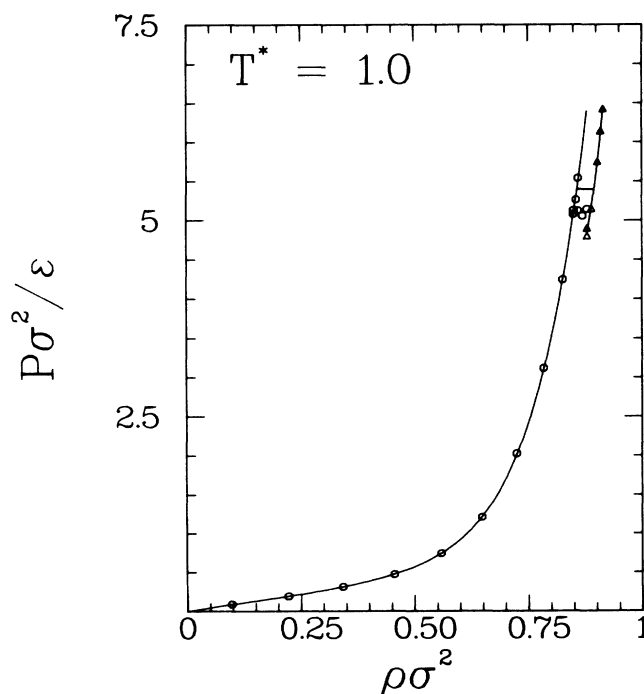


FIG. 3. Monte Carlo results for the isotherm of a 240-particle 2D LJ system at $T^*=1.00$. Meaning of symbols as in Fig. 2.

TABLE II. The free energy of the 2D LJ solid at a density $\rho^* = 0.9165$ and $T^* = 0.83$ and $T^* = 1.00$. Columns 3–5 contain the solid-liquid coexistence data, computed using these free energies.

T^*	$\beta F_{ex} (\rho^* = 0.9165)$	ρ_l^*	ρ_s^*	p^*
0.83	0.375(3)	0.831	0.870	3.42
1.00	0.914(1)	0.858	0.895	5.40

istence data and the free energies of the solid reference states have been collected in Table II. Figure 4 shows a close up of the coexistence region in Fig. 3. In Fig. 4 we have included the Monte Carlo data of Barker *et al.* to illustrate the fact that our equation of state data agree with those of Ref. 10. However, the figure clearly shows that the present polynomial fit follows the Monte Carlo data for the fluid more closely than the Padé approximant of Ref. 10. As we both use a different value for the free energy for the solid and a different fit to the pressure-pressure data of the fluid, it is not surprising that we do not find the same tieline for the solid-liquid coexistence point as reported in Ref. 10 (and reproduced in Fig. 4). Actually, there are two opposing effects. The fact that we use a

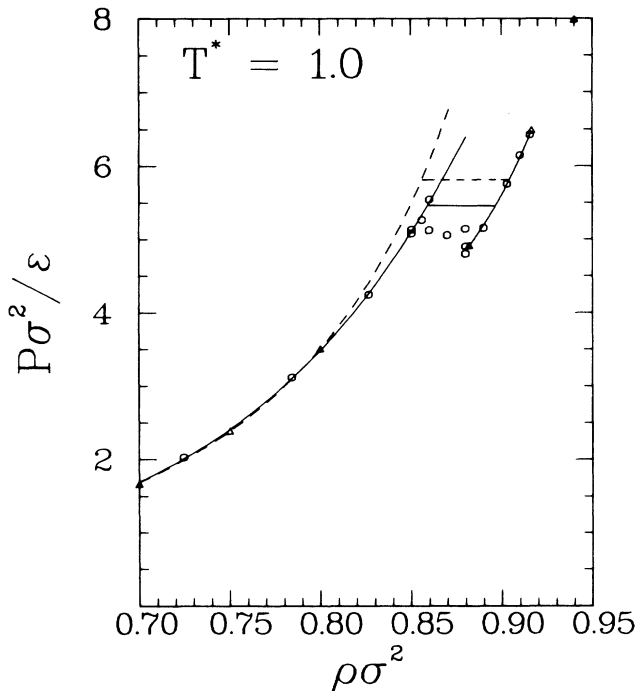


FIG. 4. Magnification of the phase transition region in Fig. 3. The dots are the Monte Carlo points. The solid curves are again the polynomial fits and the horizontal line is the tieline of the solid-liquid coexistence region. The results of Barker *et al.* (Ref. 10) are shown for comparison (triangles: Monte Carlo points; dashed curve: fit; horizontal dashed line: tieline of the coexistence region). Note that the Padé approximant of Ref. 10 fits poorly to the MC points in the vicinity of the phase transition. Note also that the tieline computed by Barker *et al.* predicts coexistence between solid and a mechanically unstable liquid.

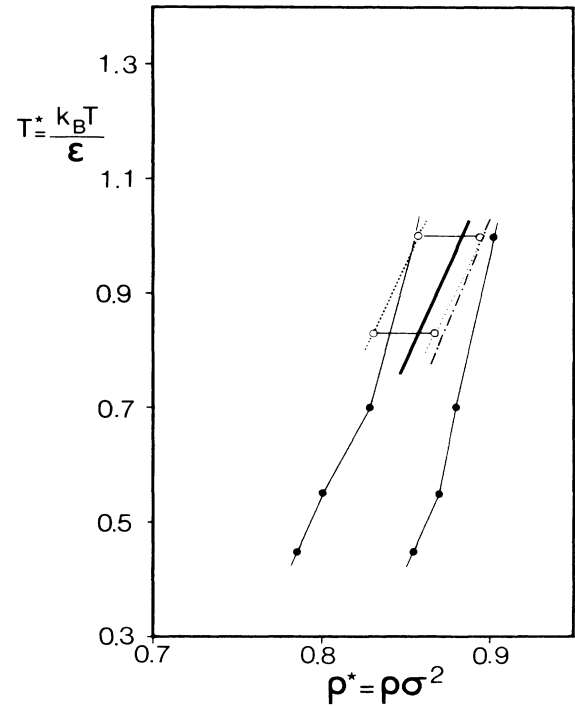


FIG. 5. The melting line of the 2D LJ system as obtained from the present calculations, compared with the phase diagram of Ref. 10. Open dots: present results. The dotted lines have been drawn as a guide to the eye. The dashed-dotted line indicates the density of the solid at melting as estimated from the large system simulations of Refs. 12 and 13. Inside the coexistence region, the locus of points where ξ_6 diverges (Refs. 6 and 13) has been indicated by a solid line.

lower pressure for the fluid tends to shift the transition to higher densities (and this is precisely what is observed by Toxvaerd⁸). However, in the present case this upward shift is more than compensated by the downward shift, which results from the fact that we use a lower value for the free energy of the solid. Figure 5 shows a section of the (ρ^*, T^*) diagram in which we compare the present estimate for the solid-fluid coexistence region with the data of Refs. 10, 12, and 13.

III. DISCUSSION AND CONCLUSIONS

The most striking feature of Fig. (5) is that the present estimate for the melting line of the solid is much closer to the points determined in molecular dynamics (MD) simulations of large systems,^{12,13} than the phase diagram published by Barker *et al.*¹⁰ In particular, we note that we find a two-phase region that is appreciably narrower than the one given in Ref. 10. At $T^* = 1.0$, Toxvaerd⁸ finds a coexistence region of approximately the same width as we do, although at a somewhat higher pressure and density. We stress once again that our equation-of-state data are consistent with those of Refs. 9 and 10. The difference with Ref. 10 resides in the fit to the equation of state of the fluid, which is clearly overestimated by the Padé approximant used by Barker *et al.* (see Fig. 4). The only difference between the present results and those of Tox-

vaerd is that we use a lower value for the excess free energy of the solid. If we had used Toxvaerd's free energy, we would have found the same coexistence points. However, the puzzling feature of the tie lines found by Toxvaerd and by Barker *et al.* is that they suggest thermodynamic coexistence between a solid and a mechanically unstable fluid. The melting line on the solid side, which results when using the free-energy values of Table II is fairly close to the large system results (Fig. 5). The remaining discrepancy is probably due to the difference in system size. We also note that estimates of the coexistence density of the liquid which follow from constant volume MD simulations on large systems^{12,13} do not agree with the present results. However, this discrepancy is not surprising. In the constant-density MD simulations, the low-density border of the coexistence region is estimated from the apparent change in slope of the equation of state. But the point where this change takes place is not very well defined.

Let us next consider how the present results compare with earlier numerical tests of the KTHNY theory of 2D melting. We recall that Abraham⁷ concluded that the stiffness constant K , which is predicted to equal 16π at the dislocation unbinding transition, was appreciably larger than this value at the melting point of the solid. If this is so, then this is a clear indication that the 2D melting transition in a Lennard-Jones system is not of the Kosterlitz-Thouless type. In contrast, Tobochnik and Chester⁶ found that in their constant density simulations the condition $K = 16\pi$ is satisfied at the point where the solid is observed to melt. Udink and van der Elsken¹³ found in constant density simulations of systems with $O(10^4)$ particles that melting coincides with the point where the exponent η , which describes the algebraic decay of translational order in the solid, crosses the upper bound $\eta = \frac{1}{3}$. The present simulations indicate that the "thermodynamic" melting line is very close to the "dislocation-unbinding" line found in constant-density simulations. So close, in fact, that we cannot use these data to confirm or refute the first-order nature of the melting transition. However, even if melting is still first order, the very fact that we are close to the KTHNY melting transition has interesting consequences for the nature of the two-phase region. We shall argue that, as a consequence, the solid-fluid coexistence region of a 2D LJ system is qualitatively different from its 3D counterpart. Before proceeding, we should point out that the physical properties of the coexistence region are of practical interest, because 2D melting at constant density can be studied experimentally.¹⁴ A better understanding of 2D melting at constant density in (large) model systems should facilitate the interpretation of such experimental data. Another situation where the knowledge of the behavior of the 2D coexistence region may be useful is in the interpretation of surface melting.¹⁵

Let us assume that melting in the 2D LJ system is a normal, first-order phase transition. In that case we should expect that in the two-phase region bulk-solid coexists with bulk-fluid. The equilibrium shape of the solid and liquid regions should be such that the interfacial energy is minimal. Hence one should expect an approxi-

mately circular patch of liquid in a homogeneous crystal or vice versa.¹⁶ Such behavior is never observed in simulations of 2D melting. The reason is that because dislocation unbinding takes place (almost) at the melting point, the bulk crystal is not stable in the coexistence region. Rather, the coexisting "solid" breaks up into crystallites due to the proliferation of grain boundaries at the melting point.¹⁷ The average linear dimensions of these crystallites are of the order of one translational correlation length. This "dispersion" of crystallites has one remarkable property: it exhibits algebraic bond-orientational order. Udink and van der Elsken¹³ carried out a finite-scaling analysis of bond order in a large 2D LJ system. This analysis showed that the 2D solid melts into a "phase" with scale-invariant bond-order correlations, at least up to the linear dimensions of the system [$O(100\sigma)$]. It is understandable that in earlier simulations this phase with algebraic bond order was tentatively identified as the "hexatic" phase. However, the term "hexatic" is used to refer to a phase which contains only few free dislocations, unlike the phase under consideration. We shall therefore avoid the use of the word "hexatic" in the present context. Still, the present phase does exhibit many of the predicted properties of the hexatic phase. In particular, it becomes unstable with respect to disclination unbinding at a universal value of the Frank constant $K_A = 72k_B T/\pi$. This corresponds to an upper limit of 0.25 for the exponent η_6 , which characterizes the decay of the bond-order correlations with distance. In Fig. 6 the temperature dependence of η_6 is shown. We have also indicated the translational order exponent η which must be less than $\frac{1}{3}$ in a stable crystalline solid. From Fig. 6 it is clear that quasi-long-range bond order disappears at a higher temperature than algebraic translational order.

Also shown in Fig. 6 is that the temperature dependence of the bond-order correlation length ξ_6 . If disclination unbinding is responsible for the transition from algebraic to short-range bond order at a temperature T^* , then the KTHNY theory predicts that ξ_6 should diverge as $\exp[b/(T - T^*)^{1/2}]$. In Fig. 6, we have plotted $1/[\ln(\xi_6)]^2$ which should be proportional to $T - T^*$. This is indeed the case, as can be seen from Fig. 6. Moreover, the estimated value $T^* = 0.93$ coincides to within the statistical error with the temperature ($T^* = 0.94$), where the algebraic exponent η_6 reaches the critical value $\frac{1}{4}$. We stress that, unlike Bakker *et al.*,¹² we find no evidence for saturation of ξ_6 at values less than the linear dimension of the system. In Fig. 5, we have used the data of Refs. 8 and 13 to construct the line where bond-orientational order becomes long ranged. This line lies inside the coexistence region, approximately at a density where a normal two-phase system should contain two-third solid and one-third liquid.

Hence, the available evidence supports the assumption that a disclination unbinding transition takes place at $T^* = 0.94(1)$. We stress that, whatever the nature of the melting transition in the 2D LJ system, it is difficult to reconcile this behavior with the assumption that 2D melting is qualitatively similar to its 3D counterpart.⁷

We are therefore left with a puzzle. The thermo-

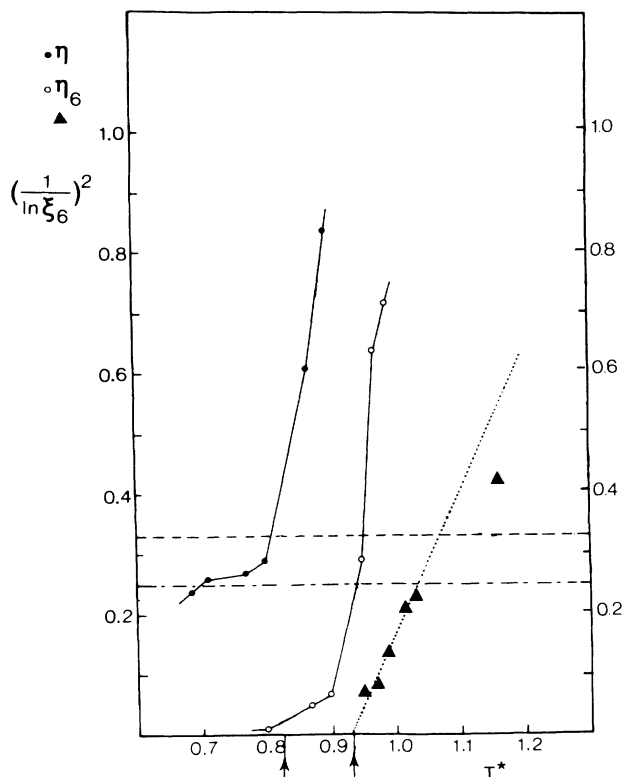


FIG. 6 Scaling results for the algebraic exponent for translational order η (solid circles) and for the algebraic exponent for orientational order η_6 (open circles) (Ref. 13). The dotted horizontal line is the critical value $\eta = \frac{1}{3}$ and the dashed-dotted horizontal line is the critical value $\eta_6 = \frac{1}{4}$. The triangles are the values of $[1/\ln(\xi_6)]^2$, with ξ_6 the orientational correlation length. The disclination unbinding theory predicts that $\xi_6 \sim \exp[b/(T - T^*)^{1/2}]$. The dotted line is a fit of $[1/\ln(\xi_6)]^2$ to $(T - T^*)/b^2$. The best fit values are $T^* = 0.93$ and $b = 0.65$. The arrows on the temperature axis indicate the translational and orientational ordering transitions, respectively.

dynamics of the melting transition in a 2D LJ system suggests a first-order phase transformation. But the “two-phase region” is highly unusual. We find no evidence for coexistence between bulk crystal and fluid. On the contrary, the intermediate phase appears homogeneous. Moreover, in the “two-phase region” we observe a clear bond-ordering transition. The phase with algebraic bond order distinguishes itself from the hexatic phase of the KTNXY theory by the fact that it is rich in defects. Yet the “critical” behavior at the bond-ordering transition suggests that we are dealing with a disclination unbinding transition of the type discussed by Halperin, Nelson, and Young. Apparently, there is more than one scenario to achieve algebraic bond order in 2D melting. We can only guess at the underlying mechanism. For instance, if we stick to the two phase coexistence picture, then the bond-ordering transition might be associated with splay rigidity percolation in a defect-rich solid, similar to the transition in a randomly diluted triangular network discussed by Wang and Brooks-Harris.¹⁸ Alternatively, the 2D solid undergoes a weak first-order transition to a defect-rich

hexatic phase. This hexatic phase then undergoes a normal disclination unbinding transition to the isotropic fluid. It maybe that neither transition is observable under conditions of constant pressure. However, as experiments on 2D melting at constant density are feasible, the nature of the region between 2D solid and isotropic fluid is of considerable interest. To our knowledge, the phase behavior revealed by the present computer simulations remains to be explained.

ACKNOWLEDGMENTS

This work is part of the research program of the Foundation for Fundamental Research of Matter (FOM), supported by the Netherlands Foundation for Chemical Research (SON), and was made possible by financial support from the Netherlands Organization for Pure Research (ZWO).

APPENDIX A

The free energy of the solid reference states with density $\rho^* = 0.9165$ for the temperatures $T^* = 0.83$ and $T^* = 1.00$ are obtained by thermodynamic integration along an artificial path. This can be done by means of a reversible change from the Hamiltonian of the Einstein crystal with the same crystallographic structure and the same temperature and density.^{19,20} To this aim we use the parametrized Hamiltonian $H(\lambda)$ (Ref. 20)

$$H(\lambda) = V_0(\mathbf{r}_0^N) + \lambda[V(\mathbf{r}^N) - V_0] + (1 - \lambda)K \sum_{i=1}^N (\mathbf{r}^i - \mathbf{r}_0^i)^2, \quad (\text{A1})$$

with V_0 the potential energy of the static lattice and $V(r)$ the potential energy of the system interacting through the Lennard-Jones potential. The last term in Eq. (A1) is the Hamiltonian of the Einstein crystal with variable spring constant: $(1 - \lambda)K$. As we know, the free energy per particle of the Einstein crystal consisting of N atoms with a fixed center of mass:

$$\beta F_E^{\text{cm}} = \left[1 - \frac{1}{N}\right] \frac{D}{2} \ln \left[\frac{\beta f}{\pi} \right] + \frac{D}{2} \frac{\ln N}{N}, \quad (\text{A2})$$

with f the spring constant $(1 - \lambda)K$ and D is the spatial dimension of the system. The excess free energy of the Einstein crystal per particle ($\lambda = 0$) is then obtained by subtracting the free energy of the ideal gas with fixed center of mass:

$$\begin{aligned} \beta F_{\text{ex}}^E &= \beta(F_E^{\text{cm}} - F_{\text{id}}^{\text{cm}}) \\ &= \left[1 - \frac{1}{N}\right] \ln \left[\left(\frac{\beta f}{\pi} \right)^{D/2} \frac{e}{\rho} \right] - \frac{3}{2} \frac{\ln N}{N} \\ &\quad + \ln \left[\frac{e}{(2\pi)^{1/2}} \right] / N + \frac{1}{N} \ln \left[\frac{6}{\pi} \right]^{D/2}. \end{aligned} \quad (\text{A3})$$

For a two-dimensional system containing 240 particles we obtain for $T^* = 0.83$ and $K = 50$, $\beta F_{\text{ex}} = 3.993$ and for $T^* = 1.00$ and $K = 150$, $\beta F_{\text{ex}} = 4.9012$. To obtain the free

energy of the system ($\lambda=1$) we evaluate

$$\Delta F = \int_0^1 \left[\frac{\partial F}{\partial \lambda} \right] d\lambda, \quad (\text{A4})$$

with

$$\left[\frac{\partial F}{\partial \lambda} \right] = \langle V(\mathbf{r}^N) - V_0 - K \sum_{i=1}^N (\mathbf{r}^i - \mathbf{r}_0^i)^2 \rangle_\lambda \quad (\text{A5})$$

in a Monte Carlo simulation. $\beta F_{\text{ex}}(240)$, the excess free energy of a system of 240 particles, is then obtained as a sum of three terms

$$\beta F_{\text{ex}}(240) = \beta F_{\text{ex}}^E(240) + \beta \Delta F(240) + \beta V_0. \quad (\text{A6})$$

The value $V_0 = -3.3767$ we used, is again calculated with the same cutoff radius and the corresponding tail correction. The resulting values for βF_{ex} ($N=240$) are given in Table II.

APPENDIX B

The free energy along the solid branch of the isotherm for densities below $\rho^* = 0.9165$ is obtained by thermodynamic integration

$$\beta F(\rho) = \beta F(0.9165) + \int_{0.9165}^{\rho} \left[\frac{\beta p}{\rho'^2} \right] d\rho'. \quad (\text{B1})$$

To perform the integration, the pressure is fitted to a polynomial of variable degree in the density. We found that for both temperatures a polynomial of degree three gave a good fit:

$$p = A_1 \rho + A_2 \rho^2 + A_3 \rho^3. \quad (\text{B2})$$

For the fluid branch the excess free energy is calculated as

$$\beta F_{\text{ex}}(\rho) = \int_0^{\rho} \left[\frac{\beta p}{\rho'} - 1 \right] / \rho' d\rho'. \quad (\text{B3})$$

Again a polynomial fit can be made:

$$p = \rho T \left[1 + B_2 \rho + \sum_{i=2}^6 A_{i-1} \rho^i \right], \quad (\text{B4})$$

where B_2 is the second virial coefficient, which was not fitted but calculated numerically. In this case five terms were needed to make a good fit. With (B4) we can write the integral in (B3) as

$$\int_0^{\rho} (B_2 + A_1 \rho' + A_2 \rho'^2 + A_3 \rho'^3 + A_4 \rho'^4 + A_5 \rho'^5) d\rho'. \quad (\text{B5})$$

In the polynomial fit (B4) we used the values $B_2(T^* = 0.83) = -1.817$ and $B_2(T^* = 1.00) = -1.073$. The value for $T^* = 1.00$ does agree with the value $f_1 - g_1$ from the table of rational approximants in Ref. 1. As the free energies are known along both branches from the above procedure, we can determine phase coexistence points from the two equations

$$p^*_{\text{solid}} = p^*_{\text{liquid}} \quad (\text{B6})$$

$$\left[F^* + \frac{p^*}{\rho^*} \right]_{\text{solid}} = \left[F^* + \frac{p^*}{\rho^*} \right]_{\text{liquid}}.$$

The resulting existence points have been collected in Table II.

¹J. M. Kosterlitz and D. J. Thouless, J. Phys. C **6**, 1281 (1973).

²D. R. Nelson and B. I. Halperin, Phys. Rev. B **19**, 2457 (1979).

³A. P. Young, Phys. Rev. B **19**, 1855 (1979).

⁴See, for example, *Ordering in Two Dimensions*, edited by S. K. Sinha (North-Holland, Amsterdam, 1980); J. Q. Broughton, G. H. Gilmer, and J. D. Weeks, Phys. Rev. B **25**, 4651 (1982); J. Tobochnik and G. V. Chester, Phys. Rev. B **25**, 6778 (1982).

⁵D. Frenkel and J. P. McTague, Phys. Rev. Lett. **42**, 1632 (1979).

⁶J. Tobochnik and G. V. Chester, Phys. Rev. B **25**, 6778 (1982).

⁷F. F. Abraham, Phys. Rev. B **23**, 6145 (1981); Phys. Rep. **80**, 339 (1980).

⁸S. Toxvaerd, Phys. Rev. A **24**, 2735 (1981).

⁹F. v. Swol, L. V. Woodcock, and J. N. Cape, J. Chem. Phys. **73**, 913 (1980).

¹⁰J. A. Barker, D. Henderson, and F. F. Abraham, Physica

106A, 226 (1981).

¹¹J. P. Hansen and L. Verlet, Phys. Rev. **184**, 151 (1969).

¹²A. F. Bakker, C. Bruin, and H. J. Hilhorst, Phys. Rev. Lett. **52**, 449 (1984).

¹³C. Udink and J. van der Elsken, Phys. Rev. B **35**, 279 (1987).

¹⁴See, for example, T. F. Rosenbaum, S. E. Nagler, P. M. Horn, and R. Clarke, Phys. Rev. Lett. **50**, 1791 (1983); W. B. Brinkman, D. S. Fisher, and D. E. Moncton, Science **217**, 693 (1982).

¹⁵J. Tallon, Phys. Rev. Lett. **57**, 1328 (1986).

¹⁶J. E. Mayer and W. W. Wood, J. Chem. Phys. **42**, 4268 (1965).

¹⁷M. P. Allen, D. Frenkel, W. Gignac, and J. P. McTague, J. Chem. Phys. **78**, 4206 (1983).

¹⁸J. Wang and A. Brooks-Harris, Phys. Rev. Lett. **55**, 2459 (1985).

¹⁹D. Frenkel and A. J. C. Ladd, J. Chem. Phys. **81**, 3188 (1984).

²⁰D. Frenkel, Phys. Rev. Lett. **57**, 1428 (1986).